Available online at www.CivileJournal.org

Civil Engineering Journal

(E-ISSN: 2476-3055; ISSN: 2676-6957)

Vol. 11, No. 06, June, 2025

Performance of Auto Glass Powder-High Calcium Fly Ash Geopolymer Mortar Exposed to High Temperature

Yuwadee Zaetang [1], Athika Wongkvanklom [1], Saengsuree Pangdaeng [2], Sakonwan Hanjitsuwan [3], Ampol Wongsa [4*], Vanchai Sata [4], Prinya Chindaprasirt [4, 5]

[1] Department of Civil and Environmental Engineering, Faculty of Science and Engineering, Kasetsart University Chalermphrakiat Sakon Nakhon Province Campus, Sakon Nakhon, 47000, Thailand.

[2] Division of Civil Engineering, Faculty of Engineering, Nakhon Phanom University, Nakhon Phanom 48000, Thailand.

[3] Department of Survey and Geomatics Engineering, Faculty of Engineering and Technology, Rajamangala University of Technology Isan, Nakhon Ratchasima 30000, Thailand.

[4] Sustainable Infrastructure Research and Development Center (SIRDC), Department of Civil Engineering, Faculty of Engineering, Khon Kaen University, Khon Kaen, 40002, Thailand.

[5] Academy of Science, Royal Society of Thailand, Dusit, Bangkok 10300, Thailand.

Received 17 January 2025; Revised 21 April 2025; Accepted 26 April 2025; Published 01 June 2025

Abstract

Waste glass enhances concrete sustainability by reducing virgin material use and recycling waste. In traditional concrete, it boosts strength through pozzolanic reactions, while in geopolymer concrete, it improves durability, insulation, and resistance to harsh conditions. This study investigated the viability of substituting auto glass powder (AGP) for high-calcium fly ash (FA) in geopolymer mortar formulations. AGP was utilized as a substitute for high-calcium FA at substitution levels ranging from 0% to 40% by weight. The study examined the physical properties, compressive strength, thermal insulation, and high-temperature performance of the geopolymer composites. The findings indicated that a higher AGP content corresponded with a reduced mortar flow, while increasing the proportion of AGP resulted in the diminished compressive strength of the geopolymer composites. Incorporating 10–20% AGP into the geopolymer mortar gave satisfactory compressive strengths (75–85%) compared to the reference mortar. Thermal conductivity testing indicated that AGP enhanced the thermal insulating properties of mortar. Notably, the compressive strength, after being exposed to 600–900°C, improved with the inclusion of the AGP. Based on XRD, the combeite crystalline phase was present in the mortars containing 20% and 40% AGP after being subjected to 900ºC. This phase contributed to the durability and stability of the material. Thus, it was confirmed that AGP not only served as a beneficial additive but also could play a crucial role in the thermal resilience of geopolymer systems.

Keywords: Waste Glass; Coal Ash; Recycled Powder; Supplementary Material; Alkali-Activated Composite.

1. Introduction

Integrating recycled glass into concrete production supports environmental sustainability by reusing waste materials and decreasing reliance on new raw materials. Incorporating glass augments cement concrete's compressive strength due to the inherent pozzolanic characteristics of glass that facilitate pozzolanic reactions and support a densely consolidated concrete matrix. The ultrafine glass powder can be used as a filler, thereby enhancing the overall

---

* Corresponding author: ampowo@kku.ac.th

http://dx.doi.org/10.28991/CEJ-2025-011-06-010

mechanical attributes of the concrete composite [1-4]. In addition to its use in traditional concrete, glass powder and other waste materials play a valuable role in geopolymer concrete, offering a reduced carbon footprint compared to traditional cement-based materials [3, 5]. Incorporating waste glass into ultra-high-performance geopolymer concrete improves workability but may reduce the compressive strength under ambient curing. However, it enhances durability, providing better strength retention in harsh environments, making it suitable for sustainable construction [6]. Replacing fly ash with recycled glass powder in geopolymer concrete led to a 3.1% reduction in compressive strength due to lower reactivity, which impeded strength development. However, substituting some of the sand with gold mine tailings improved the compressive strength through a filler effect, owing to their fine particle size [7]. The use of waste glass powder as a substitute for fly ash in the geopolymer composite significantly increased the workability and compressive strength, with an optimized waste glass powder content (10–20%) resulting in a dense and homogenous geopolymer matrix with the highest compressive strength and an acceptable compressive strength of approximately 90% compared to the reference paste sample [8]. As conventional geopolymer precursors, such as fly ash, metakaolin, and slag, are becoming scarce, waste glass powder is a good source of geopolymer precursors to supplement those of aluminosilicate materials. The integration of glass powder in geopolymer concrete could modify the microstructure by promoting the formation of strong Si-O-Si bonds, which can enhance freeze-thaw resistance and reduce thermal conductivity, contributing to improved durability and thermal performance [9-11]. These improvements increased durability, making concrete more resilient in harsh environments. Other research by Zaetang et al. [8] discovered that the incorporation of waste glass powder reduced the heavy metal leaching potential of the geopolymer composite, making it more environmentally friendly.

When cement concrete is exposed to high temperatures, the water in its pores begins to evaporate. The evaporation of water within the pores creates internal pressure, leading to cracking or spalling, which causes the surface layer to detach [12, 13]. As the temperature rises from around 400°C to 600°C, the chemical structure of concrete starts to change. Calcium silicate formed during the hydration process begins to lose strength and stability [14]. Concrete mixed with glass powder has improved fire resistance compared to regular concrete. The addition of glass enhances thermal insulation, allowing heat to disperse more slowly. Furthermore, the pozzolanic reaction of glass powder contributes to a denser microstructure, which further enhances the material's fire resistance [3].

Geopolymer concrete offers enhanced fire resistance over traditional ordinary Portland cement (OPC) concrete, largely owing to the former having distinctive chemical composition and microstructural properties [15-19]. Geopolymer composites (inorganic polymeric materials) are formed from aluminosilicate precursors, such as metakaolin, slag, and fly ash, activated with alkaline solutions. This composition allows them to withstand high temperatures and resist fire effectively. The incorporation of waste glass into geopolymer concrete has been shown to improve its fire resistance. Geopolymer mortars containing waste glass have produced major improvements in the remaining compressive strength after thermal exposure. For example, it has been reported that geopolymer composites with 20% waste glass had a residual compressive strength 165% higher than reference samples after fire resistance tests [20]. Geopolymer mortars with basalt and glass powder had improved compressive strength post-fire, particularly those with 75% basalt and 25% glass powder at temperatures up to 800°C [21]. Furthermore, the addition of waste glass positively impacts the flexural strength of geopolymer composites, contributing to their overall mechanical resilience under fire conditions [22]. However, phase transformations at elevated temperatures can lead to both beneficial and detrimental effects on a geopolymer’s mechanical properties and microstructure. Understanding these transformations is crucial for optimizing geopolymer concrete for high-temperature applications.

Another study by Chindaprasirt et al. [23] demonstrated that incorporating auto glass aggregates into geopolymer mortars could significantly strengthen the bond between the aggregates and the geopolymer matrix when exposed to an elevated temperature (900°C), with the softened glass surfaces markedly enhancing the interfacial bonding. In contrast, the present study investigated the use of auto glass powder (AGP) as a partial replacement for high-calcium fly ash in geopolymer mortars. The present research examined the influence of AGP on some physical properties, the compressive strength, the thermal insulating capacity, and the high-temperature performance of the mortars. Additionally, an XRD analysis was conducted of the geopolymer mortar after exposure to elevated temperatures to evaluate the evolution of crystalline phases resulting from the substitution with the AGP by shifting the focus from using glass aggregates as a filler to using finely ground glass powder as a substitute for fly ash. The materials, sample preparation, and testing of this work are provided in detail, followed by the results, discussion, and conclusions. The findings should provide important information for the application of AGP in high-calcium fly ash geopolymer exposed to high temperatures.

2. Materials, Sample Preparation, and Testing

2.1. Materials

Geopolymer mortars were assembled using river sand conditioned to a saturated surface dry state with a specific gravity of 2.58, fineness modulus of 3.05, unit weight of 1749 kg/m^3, and a water absorption rate of 1.21%. The liquid alkali activators consisted of a commercial-grade sodium silicate solution (57.3% H_2O, 30.3% SiO_2, and 12.3% Na_2O) and a 10 M sodium hydroxide solution. The solid precursors for the geopolymer binder were auto glass powder

(AGP) and high-calcium fly ash (FA). The AGP was produced by grinding discarded automobile windscreen glass to a particle size less than 75 µm, while the FA was sourced from an electric power plant in northern Thailand. The AGP particles were angular in shape with a rough surface, whereas the FA particles were spherical with a smooth surface (Figure 1). Table 1 and Figure 2 provide details of the chemical composition and some physical properties of both materials; the AGP had a smaller average particle size, higher surface area, and lower specific gravity than the FA. The AGP contained 68% SiO_2, 14% Na_2O, and 8% CaO. The FA was regarded as Class C fly ash according to the ASTM C618-22 standard. Figure 3 presents the XRD analysis, revealing some crystalline phases in the FA.

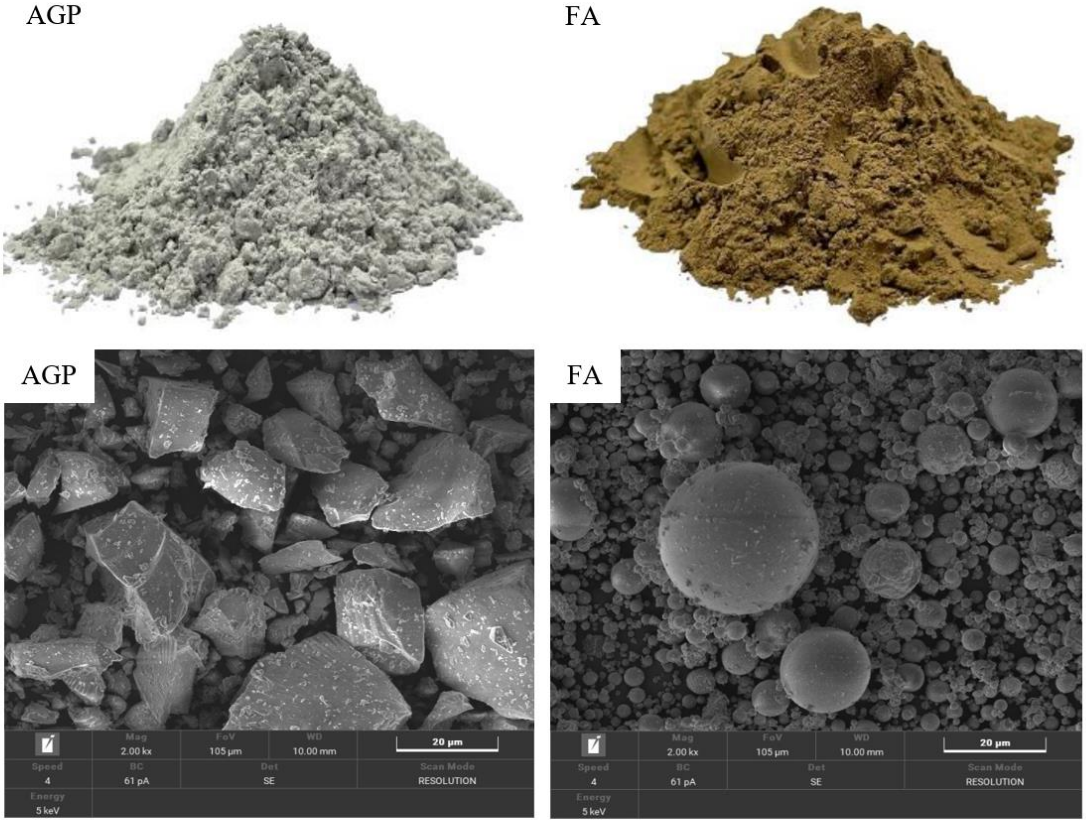

Figure 1. AGP and FA

Table 1. Chemical Constituents and Physical Attributes of AGP and FA [23]

Chemical composition (%) and physical property	AGP	FA
SiO_2	68.2	31.6
Na_2O	14.6	2.1
CaO	8.3	27.1
MgO	4.1	3.2
AlO_3	1.1	15.3
FeO_3	1.2	13.1
SO_3	0.2	3.6
K_2O	0.2	1.9
TiO_2	0.1	0.3
P_2O_5	< 0.01	0.3
Loss on ignition	2.04	1.1
Specific gravity	2.58	2.61
Mean particle size (µm)	12.6	13.3
Specific surface (BET) (m^2/g)	1.0437	1.0424
Average pore diameter (nm)	2.5155	4.0789
Total pore volume (cm^3/g)	0.0006	0.0011

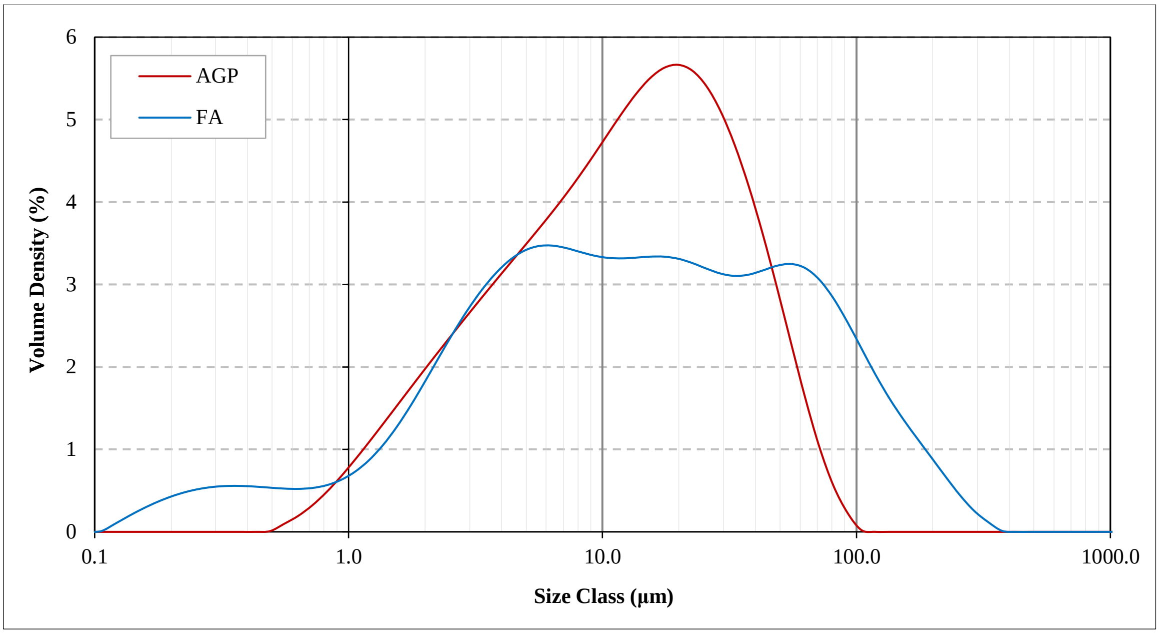

Figure 2. Particle size distribution of AGP and FA

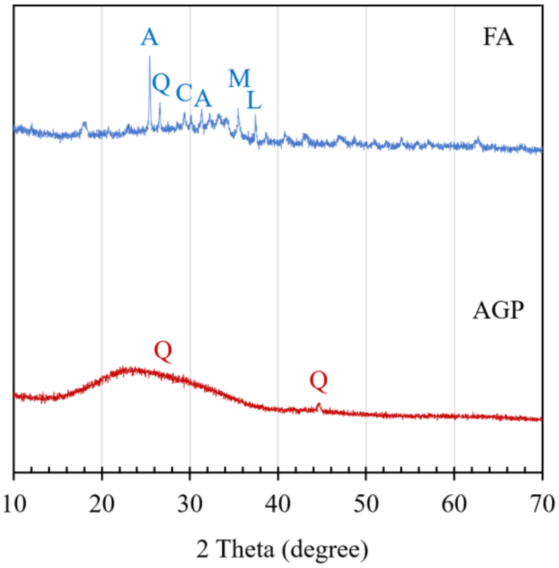

Figure 3. XRD of AGP and FA

2.2. Mix Proportions and Specimen Preparation

Five distinct mortar mixes were formulated to examine the impact on the geopolymer mortar properties of replacing FA with AGP, as outlined in Table 2. The reference mix used a sand-to-binder ratio of 2.75, a liquid-to-binder ratio of 0.58, and a sodium hydroxide-to-sodium silicate solution ratio of 1.0. The consistency rating of the reference mortar was maintained at 110±5% following the ASTM C1437-20 standard. In these mixes, FA was used instead of AGP at binder substitution levels of 0%, 10%, 20%, 30%, or 40% by weight, based on the successful use of AGP replacement levels at 10% intervals in other research by Zaetang et al. [8].

Table 2. Mix proportions

Mix	FA (g)	AGP (g)	Sodium hydroxide solution (g)	Sodium silicate solution (g)	Natural sand (g)
0AGP	1000	0	290	290	2750
10AGP	900	100	290	290	2750
20AGP	800	200	290	290	2750
30AGP	700	300	290	290	2750
40AGP	600	400	290	290	2750

Initially, the cementitious powders (FA and AGP) were combined with the sodium hydroxide solution using a pan mixer for 5 minutes. Next, natural sand conditioned to a saturated surface dry state was incorporated, followed by blending the mixture for an additional 5 minutes. Subsequently, the sodium silicate solution was introduced and blended for an additional 5 minutes. Then, the fresh mortar was cast in accordance with the ASTM C109/C109M-20 standard, to form cube specimens of two sizes (5 cm and 10 cm side lengths, respectively, called 5 cm cube and 10 cm cube throughout the text), as shown in Figure 4. To prevent moisture loss, the specimens were enveloped with a thin plastic sheet and allowed to rest at room temperature for 1 hour before undergoing a 24 hour curing process at 60°C, followed by storage in a controlled chamber at 25°C with 50% relative humidity.

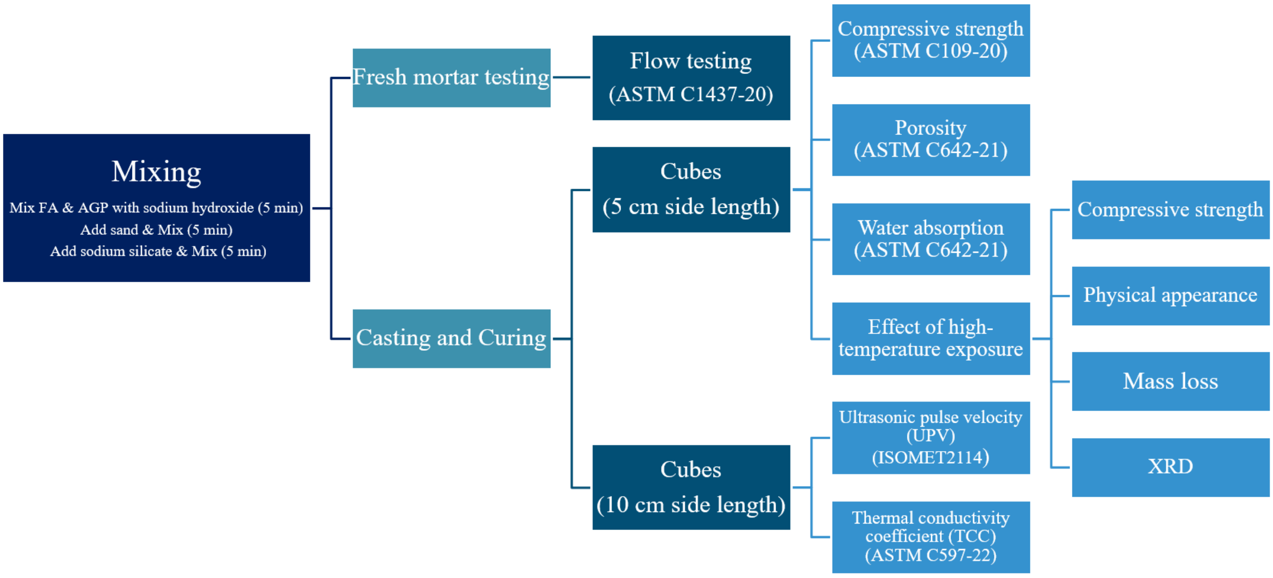

Figure 4. Procedure for mixing, casting, and testing of concrete samples

2.3. Testing

The workability of the fresh mortars was immediately assessed using flow tests in accordance with ASTM C1437-20. The compressive strength performance of the geopolymer mortar was determined using the 5 cm cube specimens at 7, 28, and 90 days following ASTM C109/C109M-20. The physical characteristics of the mortars at 28 days (porosity and water absorption) were determined according to ASTM C642-21 using the 5 cm cube specimens. The thermal conductivity coefficient (TCC) of the geopolymer mortars was tested using direct measurement with a surface probe (ISOMET2114) and the ultrasonic pulse velocity (UPV) was evaluated on the 10 cm cube specimens, in accordance with ASTM C597-22.

The impact was examined of high-temperature exposure on the compressive strength, physical appearance, and mass loss of geopolymer mortar, based on subjecting the 5 cm cube specimens at 28 days to 300˚C, 600˚C, and 900˚C. The specimens were heated to the desired temperature at a rate of 5°C per minute, maintained at that temperature for 1 hour, and then allowed to cool to ambient temperature after the furnace had been turned off.

3. Results and Discussion

3.1. Flow Values

Figure 5 illustrates the mortar flow values, which ranged from 98% to 114% and generally decreased as the AGP content increased. This decline in flow could be attributed to the angular shape of the particles, as shown in Figure 1. The FA and AGP particles had comparable particle sizes and surface areas (Table 1); however, they were notable differences in their shapes. The angular shape of AGP impeded its mobility, whereas the spherical shape of FA facilitated its motion. Other research by Khan et al. [24] reported a reduction in workability from increasing the proportion of waste glass powder as a partial substitute for low-calcium FA in alkali-activated mortars. Nevertheless, the flow values of mortars containing 10–20% AGP in the present study were still in the ١٠٥–١١٥% range. At high AGP levels (30–40%), the geopolymer mortar still had sufficient workability to ensure proper mixing, casting, compaction, and finishing of the samples. The marginal reduction in flow value could be attributed to the lower water absorption properties of the AGP than for the FA. This was supported by the lower values of average pore diameter and total pore volume of the AGP (see Table 1).

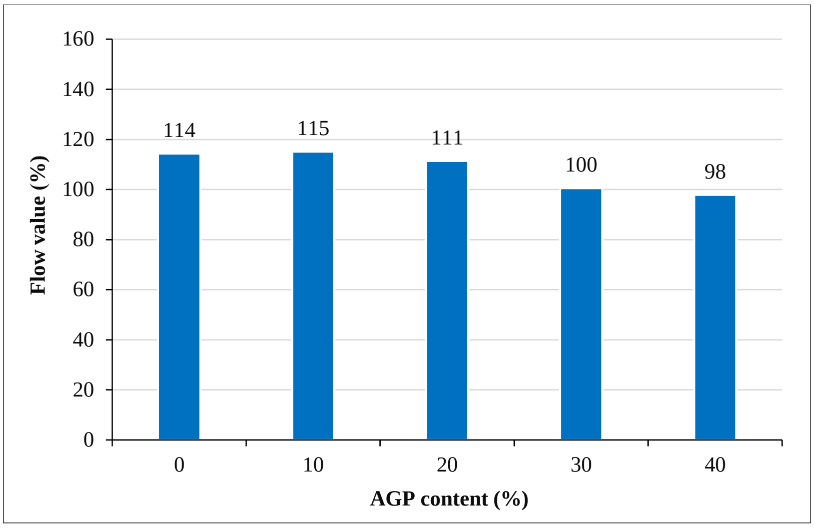

Figure 5. Flow values of geopolymer mortars

3.2. Physical Properties

Table 3 summarizes the 28 day experimental results for some physical characteristics (porosity, water absorption, and oven-dry density). These data indicated that both porosity and water absorption increased substantially with a higher AGP content because of the increased void volume due to the smooth surface and impermeable texture and the poor cohesion of glass particles to the cementitious matrix [10]. This finding aligned with Khan et al. [24], who reported that the porosity of low-calcium FA alkali-activated mortar increased as the waste glass powder content increased. Replacing low-calcium FA with waste glass powder in an alkali-activated system decelerated the reaction, leading to a higher proportion of unreacted particles and increased porosity in the geopolymer mortar composite [24]. Furthermore, Chindaprasirt et al. [23] reported that substituting natural sand with waste auto glass as the fine aggregate produced an accretion in the porosity in the high-calcium FA geopolymer mortar, with a substantial increase in water absorption associated with increasing the waste auto glass volume. As illustrated in Figure 6, the interrelationship between porosity (P) and water absorption (W) indicated that higher mortar porosity led to increased water absorption.

Table 3. Porosity, water absorption, and dry density (at 28 days)

Mix	Porosity (%)	Water absorption (%)	Dry density (kg/m^3)
0AGP	16.4	6.7	2234
10AGP	18.2	7.1	2128
20AGP	20.6	7.7	2109
30AGP	21.6	7.8	2061
40AGP	23.4	7.9	2007

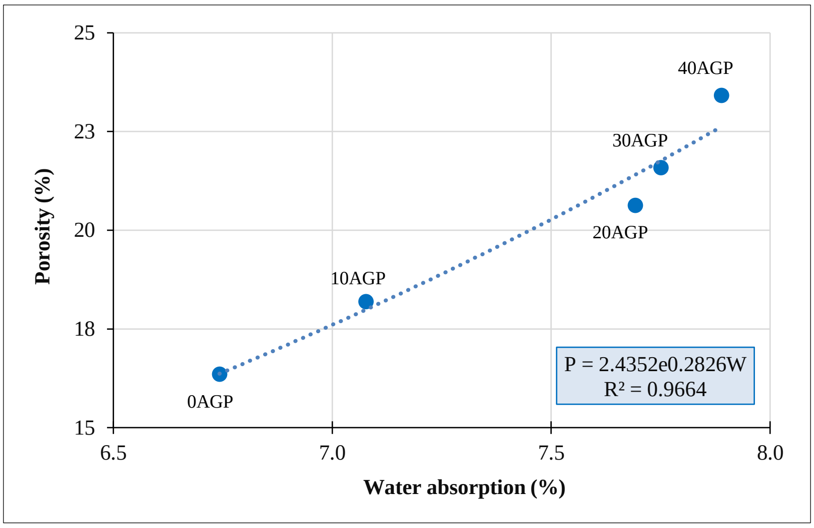

Figure 6. Relationship between porosity and water absorption

As the AGP content increased, the dry density (D) of the mortars decreased, aligning with the observed increase in porosity. Furthermore, the decrease was supported by AGP's low specific gravity compared to FA (Table 1). The density reduction in the mortar after waste glass powder inclusion has been reported in other research by Nasry et al. [4]. The density values in the dry and saturated states of the Portland cement-based mortar containing 0–60% waste glass powder from recycled soda lime glass decreased with increased partial replacement of the glass [4]. Figure 7 presents the correlation P, W, and D for the mortars examined in the present study.

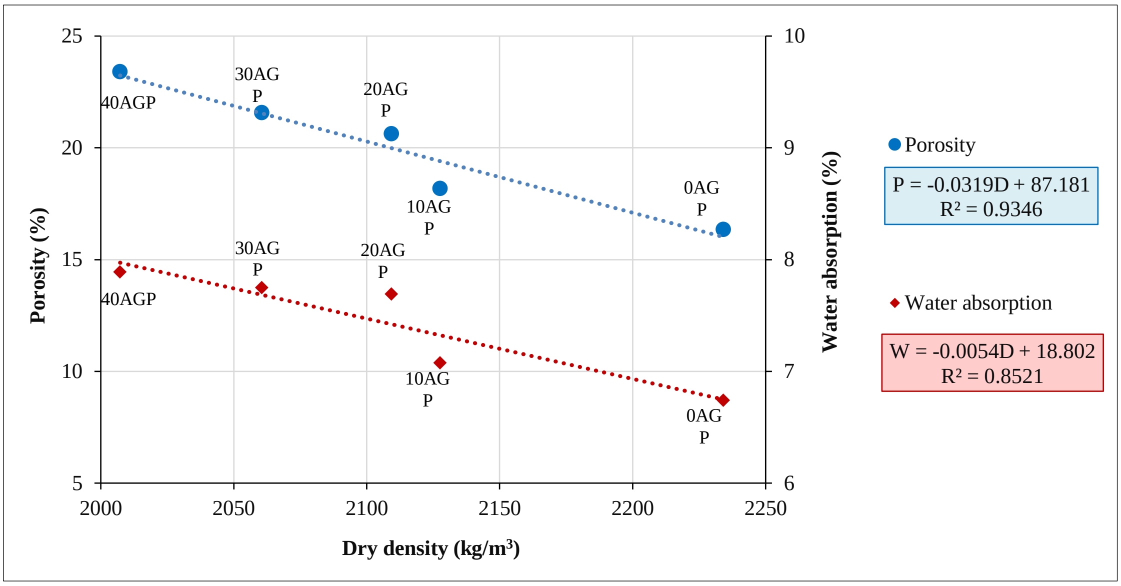

Figure 7. Relationship among porosity, water absorption, and dry density

3.3. Thermal Conductivity Coefficient and Ultrasonic Pulse Velocity

The TCC values for the geopolymer mortars mixed with 0%, 10%, 20%, 30%, or 40% AGP were 1.63, 1.54, 1.45, 1.33, and 1.32 W/mK, respectively. The TCC of the geopolymer mortars markedly declined with the increase in AGP content, with the TCC of the 40% AGP mortar being about 20% lower than for the reference geopolymer mortar. This could be attributed to the low specific gravity of AGP compared to FA and the low dry density of the geopolymer mortar with AGP compared to the reference mortar without AGP. Figure 8 shows the correlation between the TCC and dry density, with a propensity for the TCC to increase as the mortar density increased. The use of AGP as a FA replacement produced a reduction in the TCC, (Figure 9), similar to the other research [1, 4, 25] on the use of other glass waste. The TCC of paste and mortar depended on the weight of waste glass in the mixture. At the same waste glass content, the AGP in the present study had a higher thermal insulating performance than recycled waste glass powder in OPC-silica fume geopolymer mortar [25] and car windscreen powder in Portland cement paste [1]. Furthermore, the use of AGP as a powder precursor in geopolymer mortar had greater potential for thermal insulating improvement than auto glass waste aggregate as a replacement for natural sand, as reported in another study by Chindaprasirt et al. [23].

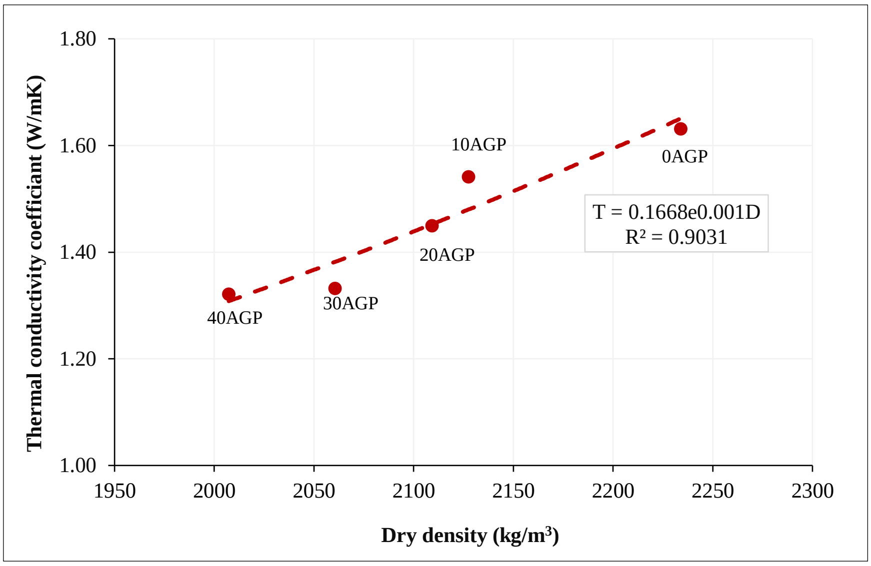

Figure 8. Thermal conductivity coefficient versus dry density

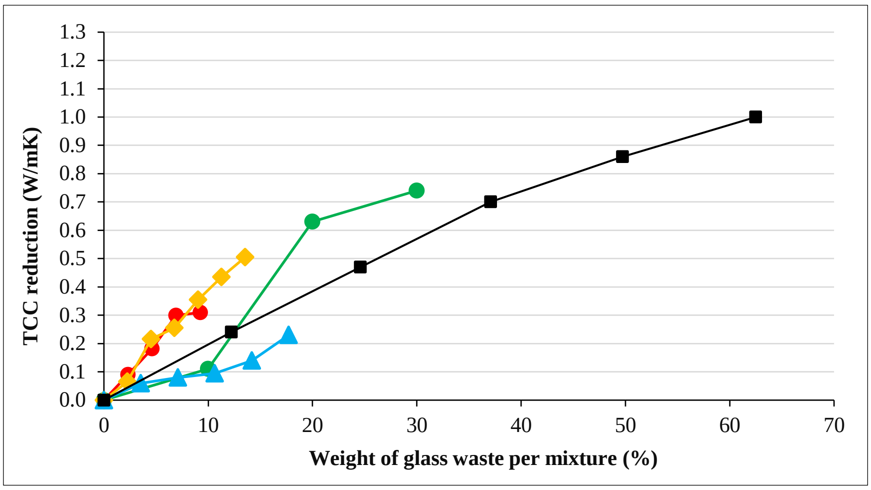

Source	Glass waste	Composite
● Present study	Auto glass powder	High-calcium fly ash geopolymer mortar
● Bostanci (2020)	Recycled waste glass powder	OPC-silica fume geopolymer mortar
◆ Nasry et al. (2021)	Soda-lime glass bottle powder	Cement mortar
▲ Du et al. (2020)	Car windscreen powder	Cement paste
■ Chindaprasirt et al. (2022)	Auto glass waste aggregate	High-calcium fly ash geopolymer mortar

Figure 9. TCC reduction versus weight of glass waste per mixture

Notably, the TCC values of mortars in the present study (1.32–1.63 W/mK) were approximately 0.37–0.68 W/mK (18–34%) lower than for OPC-based mortar (2.003 W/mK) [26] because of the low specific gravity of AGP and FA (Table 1) compared to OPC (3.15). In addition, the AGP could be used as a supplement to improve the thermal insulation performance in alkali-activated mortar and concrete applications.

The UPV values of geopolymer mortars mixed with 0%, 10%, 20%, 30%, or 40% AGP were 3931, 3734, 3630, 3346, and 3261 m/s, respectively. Increasing the AGP content generated a sizable reduction in the UPV values, attributable to the high porosity and low density of the mortars containing AGP compared to the control mix. The correlation between UPV and density values indicated that the UPV increased with increased density of the mortars. Several researchers by Farhan [27] and Naenudon et al. [28] have reported that the UPV values of FA alkali-activated mortar and concrete increased with an increase in the density because the higher density in the mortar and concrete resulted in a more uniform and less porous structure, allowing waves to travel through the specimen more quickly and thus yielding higher UPV values. Although the inclusion of AGP reduced durability parameters, such as porosity, dry density, and water absorption, the UPV measurements indicated that the overall quality remained within acceptable standards. The UPV values for geopolymer mortars decreased with increasing AGP content (Figure 10); however, mortars with 30–40% AGP still had UPV values between 3261 and 3346 m/s. According to UPV-based concrete quality classifications [28], these values fall within the medium-quality range (3000–3500 m/s), which is above the acceptable standard. The UPV of 0–20% AGP mortars (3630–3931 m/s) also met the standard for good-quality concrete (3500–4500 m/s).

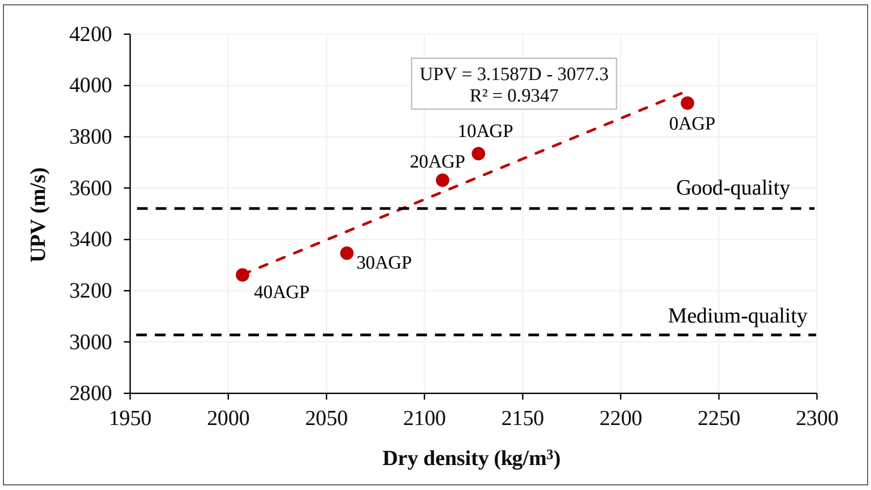

Figure 10. UPV versus dry density

3.4. Compressive Strength

Table 4 presents the compressive strength data of the geopolymer mortars. Based on these findings, the strength was influenced by both the sample age and the AGP content. The compressive strength improved with longer curing times as a result of strength development through geopolymerisation. The ٧ day compressive strength values were within the range ٩١–٩٥% of the ٢٨ day compressive strength values. This enhancement stemmed from curing at 60°C for 24 hours—a process that boosted the early-age compressive strength of the geopolymer matrix.

Table 4. Compressive strength over time

Mixture	**7 days**			**28 days**			**90 days**		
	MPa	**Std.**	**%**	**MPa**	**Std.**	**%**	**MPa**	**Std.**	**%**
0AGP	57.0	3.6	100	60.3	1.5	100	65.0	2.2	100
10AGP	49.2	3.0	86	51.2	1.5	85	53.5	3.7	82
20AGP	42.8	4.2	75	46.5	1.9	77	47.4	4.9	73
30AGP	36.2	1.9	63	37.7	2.9	62	39.6	2.4	61
40AGP	30.1	3.2	53	33.1	3.7	55	35.1	2.4	54

As the AGP content increased, the compressive strengths tended to decrease. The average compressive strengths of mortar samples containing 10%, 20%, 30%, or 40% AGP were 84%, 75%, 62%, and 54%, respectively, compared to the reference geopolymer mortar. This decline in strength could be attributed to the presence of AGP, which not only diminished the strength of the geopolymer pastes but also increased the porosity in the geopolymer mortars. In addition, other researchers [24, 29, 30] reported that the compressive strength of alkali-activated composite mixed with ground fluorescent lamp glass, container glass, and broken glass powders showed decreasing trends with an increase in the replacement levels of waste glass powder. Furthermore, Khan et al. [24] claimed that incorporating waste glass powder as a precursor at levels in the range 0–40% did not improve the compressive strength of low-calcium FA geopolymer mortars, which aligned with the present results observed in the high-calcium FA geopolymer mortars containing AGP.

Generally, the replacement of sand with waste glass aggregate in geopolymer concrete and mortar had reportedly tended to the reduce compressive strength [23, 31]. Furthermore, a comparison of the present study with previous research by Chindaprasirt et al. [23] reveals that substituting FA with AGP had a more pronounced impact on compressive strength than replacing sand with auto glass aggregate. For example, replacing only 10% of the FA with AGP resulted in compressive strengths comparable to those achieved by replacing 80% of the sand with auto glass aggregate. Although the geopolymer mortar compressive strengths in the present study declined with an increase in the AGP content, the trade-off involved balancing the AGP content to optimize insulation while maintaining acceptable strength. The use of 10–20% AGP to replace FA resulted in an acceptable compressive strength of 75–85% of the reference geopolymer mortar, while offering better thermal performance. Furthermore, the 28 day compressive strengths of the 10–20% AGP geopolymer mortar (46.5–51.2 MPa) were consistent with the range for the 28 day compressive strengths of OPC-based mortars (46.1–49.5 MPa) [26] with the same flow values (105–115 %). Figure 11 shows the good correlation (high R^2 values) between the compressive strength (C) and the UPV values of 28 day geopolymer mortars. The compressive strength rose as its UPV value increased.

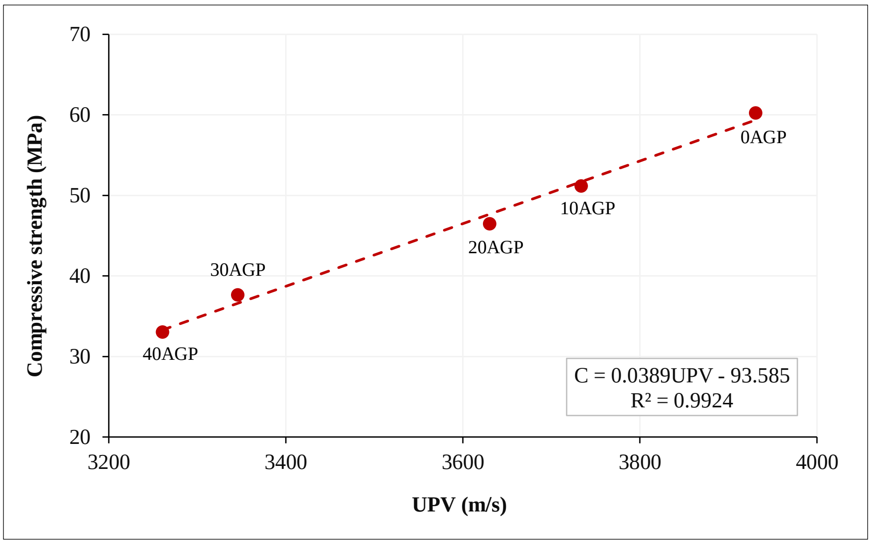

Figure 11. 28 day compressive strength versus UPV

3.5. Physical Appearances and Mass Loss of Geopolymer Mortar after High-Temperature Exposure

The physical appearances of the geopolymer mortars before and following high-temperature exposure are shown in Figure 12. At room temperature (25˚C), the color hue of the reference mortar was dark gray and dark brown, similar to the FA color (Figure 1) and changed to gray when the AGP content increased (due to the gray color of AGP). Temperature exposure shifted the reference geopolymer mortar color to a light brown hue, which was attributed to moisture loss within the geopolymer matrix that corresponded with the observed trend of increased mass loss in all the geopolymer mortars following higher temperature exposure, as shown in Figure 13. After exposure at 300°C, 600°C, and 900°C, the geopolymer mortar samples had mass losses within the ranges 7.6–7.9%, 8.1–8.4%, and 8.2–8.5%, respectively. For geopolymer mortar mixed with AGP, the gray color of the 20–40% AGP geopolymer mortar samples changed to a light gray color after 300˚C temperature exposure and to a light brownish-red color after 600˚C and 900˚C temperature exposures due to the color change caused by the melting of the AGP, as shown in Figure 14. However, there were no differences in the mass loss values of the geopolymer mortars mixed with 0–40% AGP following the same temperature exposure.

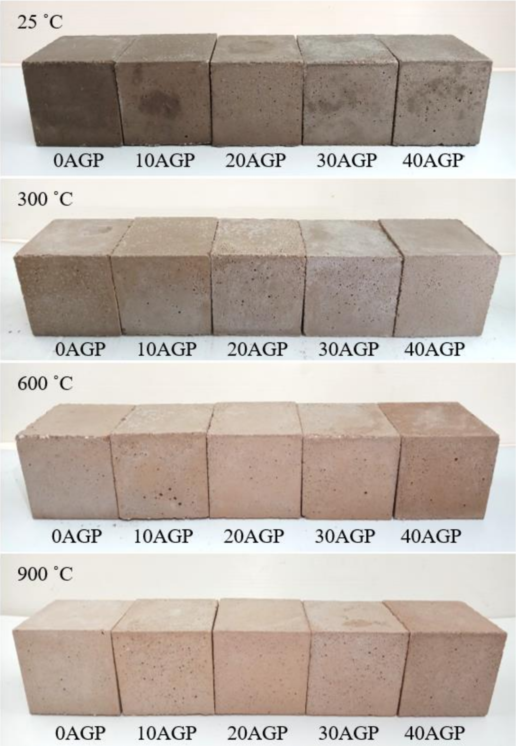

Figure 12. Geopolymer mortars after being exposed to 25˚C, 300˚C, 600˚C, and 900˚C

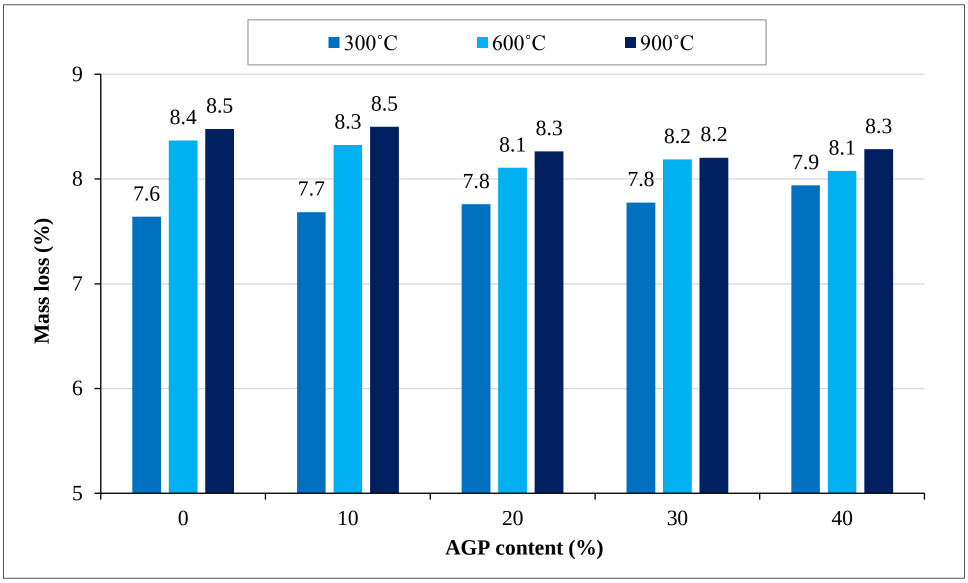

Figure 13. Mass loss of geopolymer mortar after exposures at 300˚C, 600˚C, and 900˚C

25ºC **300ºC** **600ºC** **900ºC**

Figure 14. AGP after being exposed to 25˚C, 300˚C, 600˚C, and 900˚C

3.6. Compressive Strength and XRD Analysis of Geopolymer Mortar after High-Temperature Exposure

Figure 15 illustrates the compressive strength of mortar samples, both before and after undergoing temperature exposure, along with the corresponding relative compressive strengths. Following exposure to high temperatures, the 0% AGP geopolymer had a notable decline in its compressive strength, with values after exposure to 300˚C, 600˚C, and 900˚C being 25%, 18%, and 19%, respectively, of the compressive strength before undergoing temperature exposure. These results were due to the distinct thermal expansion characteristics of the geopolymer paste compared to the sand particles [32]. Consistent with these observations, another study by Chindaprasirt et al. [23] reported a substantial decrease in the compressive strength of high-calcium FA-based geopolymer mortar as temperature exposure increased.

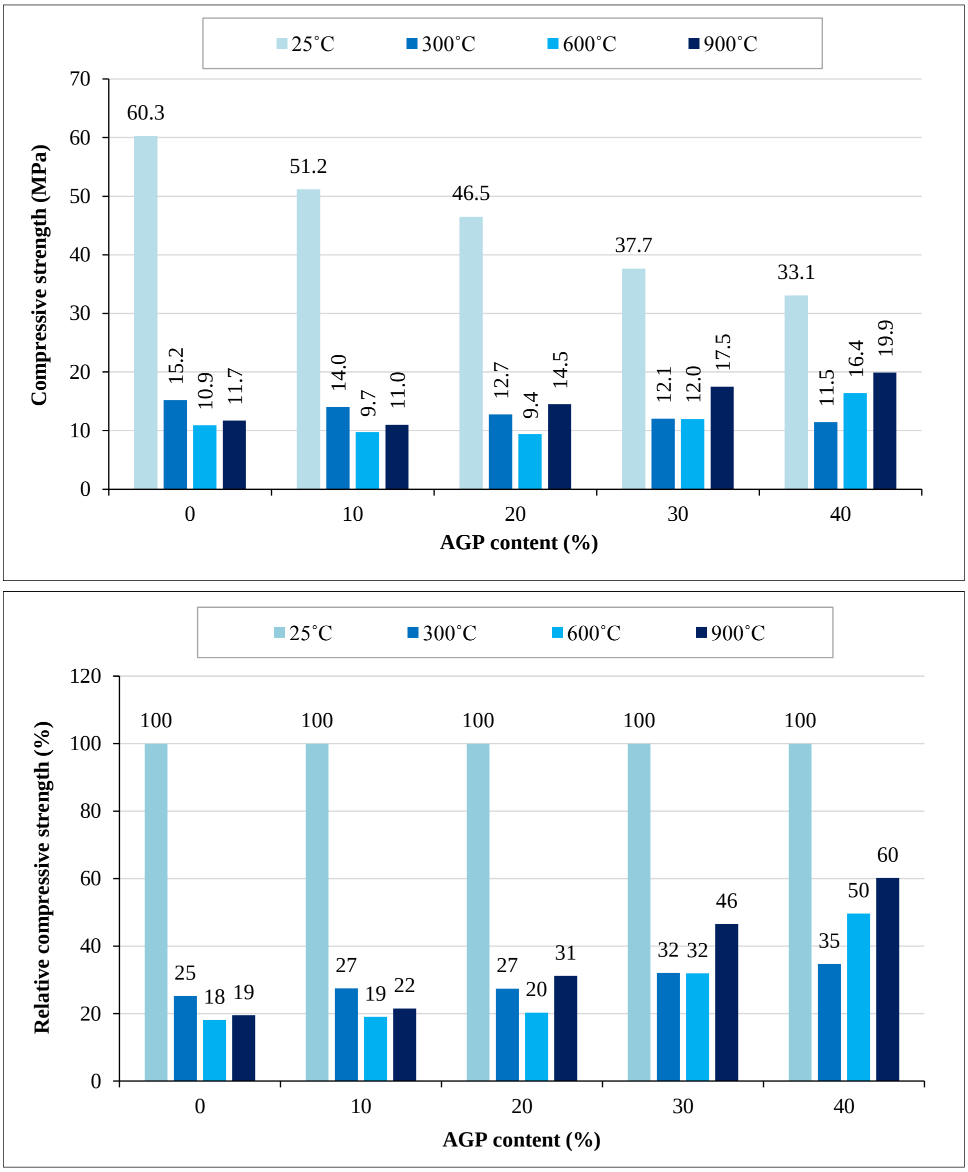

Figure 15. Compressive strength and relative strength versus AGP content of geopolymer mortar

Based on the present test results, incorporating AGP notably enhanced the fire-resistant capacity of the geopolymer mortar. The relative compressive strength increased considerably with higher AGP levels. Especially after exposure at 900°C, the relative compressive strength values for the geopolymer mortars formulated with 0%, 10%, 20%, 30%, and 40% AGP were 19%, 22%, 31%, 46%, and 60%, respectively, compared to the samples before exposure at high temperature. XRD analysis was used to investigate the improvement in the compressive strength of the mortars due to the use of AGP as FA replacement and the high-temperature exposure, as shown in Figure 16. Based on the XRD results, the quartz (SiO_2) peak was the main crystalline phase in all the geopolymer mortars before and after exposure to high temperatures due to the natural sand composition in the mortar mixture. After 900ºC exposure, notable phases were detected, including for gehlenite, nepheline, lazurite, and combeite. As the geopolymers were exposed to high heat, the crystal structures of the minerals changed, leading to the formation of new phases. Gehlenite was found in the synthetic geopolymer mortars with a notable proportion of FA (0 and 20% AGP).

The presence of calcium in the FA facilitated the formation of gehlenite at 900˚C. Klima et al. [33] concluded that adding reactive calcium to class F fly ash resulted in the precipitation of Ca-bearing minerals that contributed to the increased strength of the geopolymer. In addition, the presence of a high proportion of FA in the geopolymer matrix contributed to the formation of nepheline. FA was a by-product of coal combustion and contained a large amount of amorphous silica (SiO_2) and alumina ($Al_2 O_3$), which are essential components for the formation of nepheline in a geopolymer system. A microstructure study of methacaolin-derived geopolymer mortar revealed the formation of nepheline at 900℃ [34]. Furthermore, one study by Jiang et al. [35] claimed that the presence of nepheline proved that waste glass powder had taken part in the polymerization of the FA geopolymer paste following exposure to high temperatures (1200℃).

The inclusion of AGP in the geopolymer mortars resulted in the crystallization of the lazurite and combeite phases at high temperature. Lazurite tended to increase with an increase in the AGP content. Specifically, the combeite crystalline phase was detected only in geopolymer mortars with 20% and 40% AGP after exposure at 900°C, with the quantity increasing as the AGP content increased, resulting in enhanced compressive strength. The mechanism underlying the formation of combeite appeared to be associated with the high-temperature exposure of the mortar, during which glass particles dissolved in the alkaline systems and released sodium, calcium, and silica into the system. Subsequently, these constituents interacted and combined in appropriate proportions to form the combeite phase. In contrast, the reference geopolymer systems underwent an amorphous-to-crystalline transformation without the glass dissolution.

Other studies by Filho et al. [36] and Juraski et al. [37] reported that the combeite crystalline phase formed in Na-containing systems and was also known to develop from the crystallization of glass. Fakhruddin and Mohamad [38] reported that the combeite phase peak became more pronounced due to the enhanced crystallinity of the bioactive glass induced by a sintering temperature increase to 800°C, with the notable crystalline content playing a role in enhancing the mechanical strength due to its well-arranged atoms. This provided strong support for the resultant improved relative compressive strength and bonding of the FA-based geopolymer mortars with an AGP content after being subjected to 900°C. These findings should provide strong support for the development of fire-resistant materials utilizing geopolymer technology.

Other research has considered that the enhanced compressive strength of geopolymer mortars could be attributed melting of the AGP, which promoted the fusion and integration of the geopolymer matrix with the glass powder. Chindaprasirt et al. [23] observed that increasing the level of auto glass waste aggregate replacement substantially enhanced the relative compressive strength of FA-based geopolymer mortar following exposure at 900˚C. Similarly, Zhang et al. [39] reported that once glass waste particles reached their melting point, the molten glass filled internal cracks and voids, leading to improved bonding between the geopolymer paste and glass particles, and consequently enhancing compressive strength.

Compared to AGP, the fire-resistant performance of other refractory materials, such as ceramic fibers, steel fibers, and fiberglass, have disadvantages in terms of cost, weight, and flexibility in application. However, the choice of material depends on the intended purpose. If high heat resistance is required, refractory materials, such as steel fibers and fiberglass, remain good options. On the other hand, AGP may be a better alternative if cost savings and environmental friendliness are priorities.

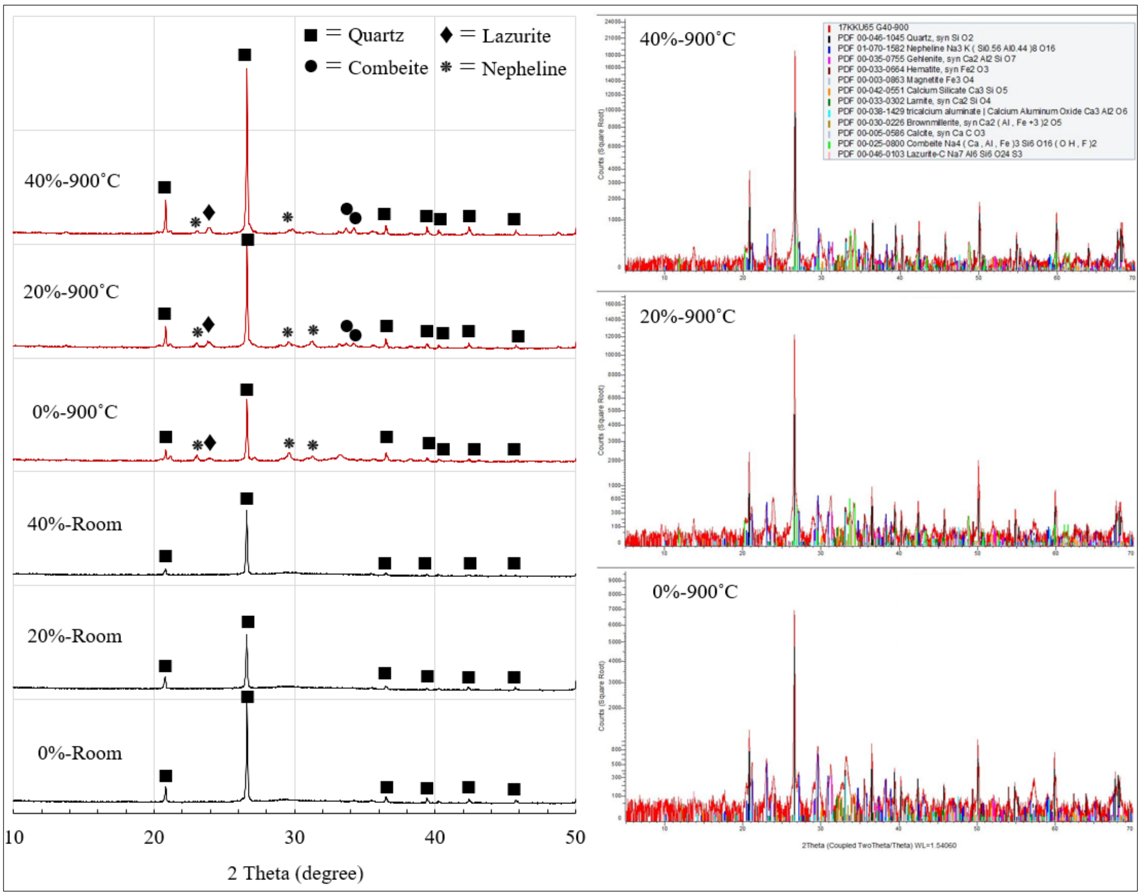

Figure 16. XRD pattern of geopolymer mortar before and after 900°C exposure

4. Conclusions

The impact was investigated of using auto glass powder (AGP) as an alternative precursor to substitute for some of the high-calcium fly ash (FA) on the compressive strength, selected physical properties, thermal insulation, and high-temperature characteristic of geopolymer mortar composites. Based on the tests of these parameters, the inclusion of AGP affected the high-calcium FA geopolymer mortar properties as follows.

- Increasing the AGP content notably reduced both the flowability and the compressive strength of the geopolymer mortars. However, incorporating 10–20% AGP into the mix maintained the compressive strength at an acceptable level (75–85%) of that of the reference mortar (without AGP).
- Based on the values for porosity, dry density, and water absorption, the durability of the mortars tended to decrease after AGP inclusion. However, the UPV testing indicated that the geopolymer mortars were still classified as good-quality concrete with 0–20% AGP inclusion in the mortar and as medium-quality concrete for 30–40% AGP mortars.
- The TCC of the geopolymer mortar notably decreased with an increase in the AGP content, with the TCC of the 40% AGP mortar being about 20% lower than the reference mortar. AGP inclusion could improve the thermal insulating characteristic of the high-calcium FA geopolymer mortars.
- The relative compressive strength values obtained after high-temperature exposure confirmed that incorporating AGP as a precursor at 600–900ºC enhanced the strength of the high-calcium FA geopolymer mortars. The inclusion of AGP in geopolymer mortars after exposure at 900ºC contributed to the formation of combeite phases, resulting in compressive strength enhancement. This study highlighted substantial prospects for applying geopolymer technology in the development of fire-resistant materials.

5. Declarations

5.1. Author Contributions

Conceptualization, Am.W. and P.C.; methodology, Am.W. and Y.Z.; validation, Y.Z., At.W., S.P., and S.H.; formal analysis, Am.W. and Y.Z.; investigation, Am.W. and Y.Z.; resources, Am.W., V.S., and P.C.; data curation, Am.W. and Y.Z.; writing—original draft preparation, Am.W. and Y.Z.; writing—review and editing, Am.W., Y.Z., V.S., and P.C.; visualization, Am.W. and Y.Z.; supervision, Am.W. and Y.Z.; project administration, Am.W. and Y.Z.; funding acquisition, Am.W. All authors have read and agreed to the published version of the manuscript.

5.2. Data Availability Statement

The data presented in this study are available on request from the corresponding author.

5.3. Funding and Acknowledgements

This study was funded by Khon Kaen University and the Fundamental Fund of Khon Kaen University.

5.4. Conflicts of Interest

The authors declare no conflict of interest.

6. References

[1] Du, Y., Yang, W., Ge, Y., Wang, S., & Liu, P. (2021). Thermal conductivity of cement paste containing waste glass powder, metakaolin and limestone filler as supplementary cementitious material. Journal of Cleaner Production, 287, 125018. doi:10.1016/j.jclepro.2020.125018.

[2] Al-jburi Najad, A. A., Hasan Kareem, J. K., Azline, N., & Ostovar, N. (2019). Waste glass as partial replacement in cement –A review. IOP Conference Series: Earth and Environmental Science, 357(1), 012023. doi:10.1088/1755-1315/357/1/012023.

[3] Siddika, A., Hajimohammadi, A., Mamun, Md., Alyousef, R., & Ferdous, W. (2021). Waste Glass in Cement and Geopolymer Concretes: A Review on Durability and Challenges. Polymers, 13(13), 2071. doi:10.3390/polym13132071.

[4] Nasry, O., Samaouali, A., Belarouf, S., Moufakkir, A., Sghiouri El Idrissi, H., Soulami, H., El Rhaffari, Y., Hraita, M., Fertahi, S. E. D., & Hafidi-Alaoui, A. (2021). Thermophysical Properties of Cement Mortar Containing Waste Glass Powder. Crystals, 11(5), 488. doi:10.3390/cryst11050488.

[5] Herbudiman, B., Subari, S., Nugraha, B., Pratiwi, I., Rinovian, A., Widyaningsih, E., Yanti, E. D., Erlangga, B. D., Jakah, J., & Roseno, S. (2024). Effect of Different Ceramic Waste Powder on Characteristics of Fly Ash-Based Geopolymer. Civil Engineering Journal (Iran), 10(2), 431–443. doi:10.28991/CEJ-2024-010-02-06.

[6] Tahwia, A. M., Heniegal, A. M., Abdellatief, M., Tayeh, B. A., & Elrahman, M. A. (2022). Properties of ultra-high performance geopolymer concrete incorporating recycled waste glass. Case Studies in Construction Materials, 17, 1393. doi:10.1016/j.cscm.2022.e01393.

[7] Dey, A., Rumman, R., Wakjira, T. G., Jindal, A., Bediwy, A. G., Islam, M. S., Alam, M. S., Al Martini, S., & Sabouni, R. (2024). Towards net-zero emission: A case study investigating sustainability potential of geopolymer concrete with recycled glass powder and gold mine tailings. Journal of Building Engineering, 86, 108683. doi:10.1016/j.jobe.2024.108683.

[8] Zaetang, Y., Thongrit, P., Phoo-Ngernkham, T., Tippayasam, C., Phungsai, P., Wongsa, A., Sata, V., & Chindaprasirt, P. (2025). High calcium fly ash-auto glass powder alkali-activated pastes. International Journal of Sustainable Engineering, 18(1), 2466475. doi:10.1080/19397038.2025.2466475.

[9] Çelik, A. İ., Tunç, U., Bahrami, A., Karalar, M., Othuman Mydin, M. A., Alomayri, T., & Özkılıç, Y. O. (2023). Use of waste glass powder toward more sustainable geopolymer concrete. Journal of Materials Research and Technology, 24, 8533–8546. doi:10.1016/j.jmrt.2023.05.094.

[10] Dong, W., Li, W., & Tao, Z. (2021). A comprehensive review on performance of cementitious and geopolymeric concretes with recycled waste glass as powder, sand or cullet. Resources, Conservation and Recycling, 172, 105664. doi:10.1016/j.resconrec.2021.105664.

[11] Sheng, Z., Zhu, B., Cai, J., Han, J., Zhang, Y., & Pan, J. (2024). Influence of waste glass powder on printability and mechanical properties of 3D printing geopolymer concrete. Developments in the Built Environment, 20, 100541. doi:10.1016/j.dibe.2024.100541.

[12] Sideris, K. K. (2007). Mechanical Characteristics of Self-Consolidating Concretes Exposed to Elevated Temperatures. Journal of Materials in Civil Engineering, 19(8), 648–654. doi:10.1061/(asce)0899-1561(2007)19:8(648).

[13] Willam, K., Rhee, I., & Xi, Y. (2005). Thermal Degradation of Heterogeneous Concrete Materials. Journal of Materials in Civil Engineering, 17(3), 276–285. doi:10.1061/(asce)0899-1561(2005)17:3(276).

[14] Ulm, F.-J., Acker, P., & Lévy, M. (1999). The “Chunnel” Fire. II: Analysis of Concrete Damage. Journal of Engineering Mechanics, 125(3), 283–289. doi:10.1061/(asce)0733-9399(1999)125:3(283).

[15] Jochem, L. F., Casagrande, C. A., Onghero, L., Venâncio, C., & Gleize, P. J. P. (2021). Effect of partial replacement of the cement by glass waste on cementitious pastes. Construction and Building Materials, 273, 121704. doi:10.1016/j.conbuildmat.2020.121704.

[16] Yong, H. C., Ming, L. Y., Al Bakri Abdullah, M. M., & Hussin, K. (2015). Fire resistant properties of geopolymers: A review. Key Engineering Materials, 660, 39–43. doi:10.4028/www.scientific.net/KEM.660.39.

[17] Mohd Ali, A. Z., & Sanjayan, J. (2016). The spalling of geopolymer high strength concrete wall panels and cylinders under hydrocarbon fire. MATEC Web of Conferences, 47, 2005. doi:10.1051/matecconf/20164702005.

[18] Vickers, L., van Riessen, A., & Rickard, W. D. A. (2015). Fire-Resistant Geopolymers. SpringerBriefs in Materials. Springer Singapore. doi:10.1007/978-981-287-311-8.

[19] Manzoor, T., Bhat, J. A., & Shah, A. H. (2024). Performance of geopolymer concrete at elevated temperature − A critical review. Construction and Building Materials, 420, 135578. doi:10.1016/j.conbuildmat.2024.135578.

[20] Ziejewska, C., Grela, A., Mierzwiński, D., & Hebda, M. (2023). Influence of Waste Glass Addition on the Fire Resistance, Microstructure and Mechanical Properties of Geopolymer Composites. Materials, 16(17), 6011. doi:10.3390/ma16176011.

[21] Yurt, Ü., Çelikten, S., & Atabey, İ. İ. (2024). Post-fire residual mechanical and microstructural properties of waste basalt and glass powder-based geopolymer mortars. Journal of Building Engineering, 94, 109941. doi:10.1016/j.jobe.2024.109941.

[22] Valanides, M., Aivaliotis, K., Oikonomopoulou, K., Fikardos, A., Savva, P., Sakkas, K., & Nicolaides, D. (2024). Geopolymerization of Recycled Glass Waste: A Sustainable Solution for a Lightweight and Fire-Resistant Material. Recycling, 9(1), 16. doi:10.3390/recycling9010016.

[23] Chindaprasirt, P., Lao-un, J., Zaetang, Y., Wongkvanklom, A., Phoo-ngernkham, T., Wongsa, A., & Sata, V. (2022). Thermal insulating and fire resistance performances of geopolymer mortar containing auto glass waste as fine aggregate. Journal of Building Engineering, 60, 105178. doi:10.1016/j.jobe.2022.105178.

[24] Khan, M. N. N., Kuri, J. C., & Sarker, P. K. (2021). Effect of waste glass powder as a partial precursor in ambient cured alkali activated fly ash and fly ash-GGBFS mortars. Journal of Building Engineering, 34. doi:10.1016/j.jobe.2020.101934.

[25] Bostanci, L. (2020). Effect of waste glass powder addition on properties of alkali-activated silica fume mortars. Journal of Building Engineering, 29. doi:10.1016/j.jobe.2019.101154.

[26] Naenudon, S., Vilaivong, A., Zaetang, Y., Tangchirapat, W., Wongsa, A., Sata, V., & Chindaprasirt, P. (2022). High flexural strength lightweight fly ash geopolymer mortar containing waste fiber cement. Case Studies in Construction Materials, 16, 1121. doi:10.1016/j.cscm.2022.e01121.

[27] Farhan, N. A., Sheikh, M. N., & Hadi, M. N. S. (2019). Investigation of engineering properties of normal and high strength fly ash based geopolymer and alkali-activated slag concrete compared to ordinary Portland cement concrete. Construction and Building Materials, 196, 26–42. doi:10.1016/j.conbuildmat.2018.11.083.

[28] Naenudon, S., Wongsa, A., Ekprasert, J., Sata, V., & Chindaprasirt, P. (2023). Enhancing the properties of fly ash-based geopolymer concrete using recycled aggregate from waste ceramic electrical insulator. Journal of Building Engineering, 68. doi:10.1016/j.jobe.2023.106132.

[29] Tho-In, T., Sata, V., Boonserm, K., & Chindaprasirt, P. (2016). Compressive strength and microstructure analysis of geopolymer paste using waste glass powder and fly ash. Journal of Cleaner Production, 172, 2892–2898. doi:10.1016/j.jclepro.2017.11.125.

[30] Manikandan, P., Natrayan, L., Duraimurugan, S., & Vasugi, V. (2022). Influence of Waste Glass Powder as an Aluminosilicate Precursor in Synthesizing Ternary Blended Alkali-Activated Binder. Silicon, 14(13), 7799–7808. doi:10.1007/s12633-021-01533-2.

[31] Subhani, M., Ali, S., Allan, R., Grace, A., & Rahman, M. (2024). Physical and mechanical properties of self-compacting geopolymer concrete with waste glass as partial replacement of fine aggregate. Construction and Building Materials, 437, 136956. doi:10.1016/j.conbuildmat.2024.136956.

[32] Ranjbar, N., Mehrali, M., Alengaram, U. J., Metselaar, H. S. C., & Jumaat, M. Z. (2014). Compressive strength and microstructural analysis of fly ash/palm oil fuel ash based geopolymer mortar under elevated temperatures. Construction and Building Materials, 65, 114–121. doi:10.1016/j.conbuildmat.2014.04.064.

[33] Klima, K. M., Schollbach, K., Brouwers, H. J. H., & Yu, Q. (2022). Thermal and fire resistance of Class F fly ash based geopolymers – A review. Construction and Building Materials, 323. doi:10.1016/j.conbuildmat.2022.126529.

[34] Kuenzel, C., Grover, L. M., Vandeperre, L., Boccaccini, A. R., & Cheeseman, C. R. (2013). Production of nepheline/quartz ceramics from geopolymer mortars. Journal of the European Ceramic Society, 33(2), 251–258. doi:10.1016/j.jeurceramsoc.2012.08.022.

[35] Jiang, X., Xiao, R., Ma, Y., Zhang, M., Bai, Y., & Huang, B. (2020). Influence of waste glass powder on the physico-mechanical properties and microstructures of fly ash-based geopolymer paste after exposure to high temperatures. Construction and Building Materials, 262, 120579. doi:10.1016/j.conbuildmat.2020.120579.

[36] Filho, O. P., Latorre, G. P., & Hench, L. L. (1996). Effect of crystallization on apatite-layer formation of bioactive glass 45S5. Journal of Biomedical Materials Research, 30(4), 509–514. doi:10.1002/(SICI)1097-4636(199604)30:4<509::AID-JBM9>3.0.CO;2-T.

[37] Juraski, A. D. C., Rodas, A. C. D., Elsayed, H., Bernardo, E., Soares, V. O., & Daguano, J. (2017). The in vitro bioactivity, degradation, and cytotoxicity of polymer-derived wollastonite-diopside glass-ceramics. Materials, 10(4), 425. doi:10.3390/ma10040425.

[38] Fakhruddin, A. K., & Mohamad, H. (2022). Effect of sintering temperature on mechanical and bioactivity properties of bioactive glass and cordierite composite. Ceramica, 68(385), 13–23. doi:10.1590/0366-69132022683853141.

[39] Zhang, B., He, P., & Poon, C. S. (2020). Improving the high temperature mechanical properties of alkali activated cement (AAC) mortars using recycled glass as aggregates. Cement and Concrete Composites, 112, 103645. doi:10.1016/j.cemconcomp.2020.103654.